SEAIQHRDP mathematical model Analysis for the transmission dynamics of COVID-19 in India

M. Ankamma Rao[1] and A.Venkatesh[2*]

[1,2]Department of Mathematics,
AVVM Sri Pushpam College (Affiliated to Bharathidasan University),
Poondi, Thanjavur(Dt), Tamilnadu, India-613 503.

December 28, 2022

Abstract

Mathematical modeling is one of the most used techniques for analyzing and preventing the transmission of COVID-19. To control this pandemic, it is essential to classify the infected population. So in this article, a new SEAIQHRDP model was formulated to investigate the transmittal dynamics of COVID-19. This model contains nine compartments Susceptible(S) class, Exposed(E) class, Asymptomatic(A) class, Infected(I) class, Quarantined(Q) class, Hospitalized(H) class, Recovered(R) class, Death(D) class, and Insusceptible (P) class. This model was fitted to the daily and cumulative confirmed COVID-19 cases in the period between 30^{th} January 2020 and 13^{th} January 2021 in India. Sensitivity analysis concerning R_0 was performed to classify the significance of parameters. Contour plots for R_0 were executed and the effect of various parameters on the infected classes had shown graphically. The necessity of stringent face mask usage and social seclusion is highlighted by optimal control analysis as a key factor in the dramatic reduction of infection rates. So the optimal control technique was adopted to lessen the disease mortality by taking both nonpharmaceutical and pharmaceutical intervention strategies as control functions and comparing infectives and recoveries with and without controls.

Keywords: : mathematical model, Stability analysis, Basic reproduction number, Sensitivity analysis, optimal strategy
Subject Classification: 00A71

1 Introduction

The world has been trembling with a new infectious disease COVID-19. The World Health Organization (WHO) has declared it was a universal pandemic on 11^{th} March 2020 [14]. originally The COVID-19 disease was revealed in December 2019 in Wuhan, Hubei, China. Later it increased rapidly and spread in all countries in the world. As of August 28^{th}, 2022, the total confirmed cases of 596,873,121 and death cases of 6,459,684 of COVID-19 had been reported to WHO [15]. On January 30^{th}, 2020 the first COVID-19 case [28] was placed in Kerala, India. A total of 44,389,176 confirmed cases and 527,556

*Corresponding author: avenkateshmaths@gmail.com

death cases were placed in India as of August 28^{th}, 2022. Initially, some countries implemented strictly non-pharmacological interventions namely as use of face masks social distancing, and hygiene to resist the extent of the COVID-19 pandemic. Due to these safety measures, the virus spread slowed down gradually but not ceased completely. Since the vaccination process had started, the COVID-19 cases decreased day by day and it became under control. But still now in some countries COVID- cases raises unexpectedly.

Mathematical modeling is a prominent technique for forecasting and controlling the transmission dynamics of epidemic diseases. Alexander Krämeret al.[1] H.W. Hethcote [16], R.M.May & R.M Anderson, [38] Brauer F & Chavez CC) [6]. Some standard mathematical models such as SIR, SEIR, SEIAR, SEIRD, etc. were broadly used to estimate the future trend of a pandemic. The standard SIR model Kermack WO & McKendrick [20] described the spread of the virus using the compartments of susceptible, infected, and recovered. By incorporating the new compartments, we get new models to detect the communication dynamics of contagious diseases. An SEIR model by Mwalili S et al. cite 26 was developed by adding an Exposed compartment to the SIR model which contained distinctive reaction and administration activity factors. This model is used widely to forecast the direction of the COVID-19 graph in China among other countries. Through the SEIR model, the influence of control strategies was studied by Lin Q et al.[22] and formulated the SEIR extension model. A generalized SEIR model Read JM et al.[34] was advanced in the latent period to cover the communication dynamics of COVID-19. During the incubation period, it consists of one more compartment as asymptomatic individuals in the SEIR model. The isolated class in SEIJR was interchanged with the asymptomatic class in SEIAR. By using this model, Bailey et al [2] displayed related properties to the SEIJR model Peng L et al. [30]. General models such as SIR, SEIR, SEIRD, SEIJR, etc. were not suitable for forecast the effect of the widespread disease since they comprise a finite number of parameters and disregarded essential classes such as asymptomatic infected, quarantine, Hospitalization, etc. SIDARTHE model of Giordano et al.[11] is an extension of the SEIR model which consists of undetected as well as detected infected populations.

The field of FDEs has developed greatly over the past few decades as a result of its applicability in numerous branches of research and technology. To study malaria transmission, Rehman, Attiq ul, and colleagues devised a 9 compartment FDE model [35]. By considering both the government's activity and the individual's response, Danane, Jaouad et al.[8] established a seven-compartment FDE model. Supriya, Yadav, and colleagues [42] created the FDE model to investigate the COVID-19 trend using an effective and potent analytical q-HASTM approach. By Jagdev Singh, a fractional guava fruit model with memory effect was developed [41]

In general, before showing any symptoms an individual exposed to the virus will become infectious i.e. pre-symptomatic through an incubation period of 5 days Liu C et al. [23]. Many reports have shown that a huge number of individuals who were exposed to the virus did not show any symptoms i.e., they all remain asymptomatic. The pre-symptomatic or asymptomatic individuals were capable to diffuse the virus to others. Since the reported asymptomatic cases in India are high, it was necessary to include the asymptomatic class in the epidemiological model. As for the total of parameters and accurateness model, the above-discussed models were not perfect for long-term predictions. Therefore one more compartment dead population had been incorporated in the SEIAR model presented through Huang et al.[15] to improve the accurateness model for long-term prediction.

Raj Kishore et.al [33] developed the SEIQRDP model by including the quarantine class (Q) and insusceptible class (P) and predicted the number of active cases. By

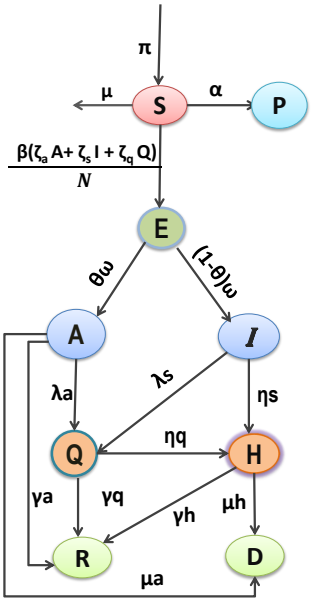

Figure 1: Flow Chart of SEAIQHRDP model

incorporating an asymptomatic class Singh HP et al [39] introduced the SEAIQRDT model and forecast the confirmed cases. When the best optimal control technique is used early in a pandemic, the intensity of epidemic peaks tends to decline, spreading the maximum impact of an epidemic across a longer time. Massad, Eduardo et al [25] developed an optimal control model to analyze the effect of vaccination on the zika virus. To analyze the COVID-19 trend in the future, Bandekar SR and Minighosh [3] devised an 11 compartments mathematical model. They then employed an optimal control strategy to reduce the disease fatality.

By taking into account all of the aforementioned discussions, We developed a new SEAIQHRDP model by including a new class—hospitalization—to the SEAIQRDP model in order to examine the transmission of COVID-19. Later an optimal control strategy with three control variables was applied to the proposed model to moderate the outspread of COVID-19 optimally.

The following sections in this manuscript were systematized as follows: SEAIQHRDP model formulation was presented in section 2. In section 3 The elementary properties of the recommended model such as positivity and boundedness, disease-free equilibrium's local stability, and R_0 expression in various parameters were executed. Section 3 finished Parameter estimation, model fitting, and model justification. Sect.5 performed the sensitive analysis concerning R_0 and the impact of parameters on infected populations. Section 6 implemented and solved an optimal control problem analytically. The work ends with the conclusion in Section 7

2 Model formation

By considering all the above discussions, in this study, a new mathematical model SEAIQHRDP was formulated. In this model, the class S(t) contained the susceptible individuals at time t, the class E(t) contained exposed individuals (these were contaminated but does not contaminate others within the reaction time), the class A(t)

contained asymptomatic infected individuals (despite no symptoms appeared in them but capable to infect others), the class I(t) contains the symptomatic individuals (these persons having symptoms and were capable to infect others), the class Q(t) contained the quarantined individuals (these were infected but isolated), the class H(t) contained the hospitalization individuals (these were infected and undergo medical treatment), the class R(t) contained the recovered individuals, the class D(t) contained the death individuals, and the class P(t) contained the insusceptible individuals those are incapable of getting infected due to either pre-isolated or following the WHO rules strictly.

Let Λ and μ be the constant recruitment rate and normal death rate in the susceptible population. Let β be the virus contact rate. Let ζ_a, ζ_q, and ζ_s be the adjustment factors for asymptomatic infected, symptomatic infected, and quarantine populations. $\beta\zeta_a$, $\beta\zeta_q$ and $\beta\zeta_h$ were the virus transmission factors of asymptomatic, symptomatic, and quarantine populations to susceptible populations. These were time-dependent factors in computations. This model has the potency of disease is $\triangle = \frac{\zeta_a A + \zeta_s I + \zeta_q Q}{N}$.

Let α be the protection rate at which the susceptible individuals move to insusceptible individuals. This included the influence of control measures. Let θ be the fraction at which the exposed individuals move to asymptomatic individuals. Then $(1-\theta)$ is the fraction at which exposed individuals move to symptomatic infected individuals at a velocity ω. Let λ_a and λ_s be the quarantine rates at which the asymptomatically infected individuals and symptomatically infected individuals were quarantined. Let η_s and η_q hospitalization rates at which the symptomatic and quarantine populations had certain complications due to severe symptoms shall be hospitalized. Let γ_a, γ_q, and γ_h be the recovery rates at which the asymptomatic infected, quarantined, and hospitalized individuals were recovered from the disease. There will be a possibility to die, in asymptomatic individuals before getting symptoms and after admitting to the hospital. Let μ_a and μ_h be the mortality rates of asymptomatic and hospitalized individuals. By using all the above conditions, The relation between these nine compartments and corresponding parameters were shown in Figure.1 and table 1

The arrangement of nonlinear differential equations for the proposed model in India was

$$\frac{ds}{dt} = \Lambda - \beta \triangle S - (\alpha + \mu)S \tag{1.1}$$

$$\frac{dE}{dt} = \beta \triangle S - (\omega + \mu)E \tag{1.2}$$

$$\frac{dA}{dt} = \theta\omega E - (\lambda_a + \gamma_a + \mu_a + \mu)A \tag{1.3}$$

$$\frac{dI}{dt} = (1-\theta)\omega E - (\lambda_s + \eta_s + \mu)I \tag{1.4}$$

$$\frac{dQ}{dt} = \lambda_a A + (\lambda_s I - (\eta_q + \gamma_q + \mu)Q \tag{1.5}$$

$$\frac{dH}{dt} = \eta_s I + \eta_q Q - (\gamma h + \mu_h + \mu)H \tag{1.6}$$

$$\frac{dR}{dt} = \gamma_a A + \gamma_q Q + \gamma_h H - \mu R \tag{1.7}$$

$$\frac{dD}{dt} = \mu_a A + \mu_h H \tag{1.8}$$

$$\frac{dP}{dt} = \alpha S. \tag{1.9}$$

with non negative primary conditions are $S(0) = S_0$, $E(0) = E_0$, $A(0) = A_0$, $I(0) == I_0$, $Q(0) = Q_0$, $H(0) = H_0$,$R(0) = R_0$, $D(0) = D_0$and $P(0) = P_0$.

Table 1: SEAIQHRDP model parameter's complete depiction.

parameter	description
Λ	Recruitment rate of human
θ	Proportion of exposed individuals
ω	Conversion rate of exposed to asymptomatically infected populace
α	Protection rate of susceptible individuals to insusceptible populace
ζ_a,ζ_s,ζ_q	Adjustment factor for asymptomatic, symptomatic and quarantine populace
β	Transmission rate of virus
λ_a	Quarantine rate of asymptomatic infected populace
λ_s	Quarantine rate of symptomatic infected populace
η_s	Hospitalization rate of symptomatic infected populace
η_q	Hospitalization rate of quarantine infected populace
γ_a	The rate of recovery from asymptomatic infected populace
γ_q	The rate of recovery from quarantine populace
γ_h	The rate of recovery from hospitalization populace
μ_a	The rate of mortality from asymptomatic populace
μ_h	The rate of mortality from hospitalization populace
μ	Normal mortality rate of human populace

3 SEAIQHRDP model analysis

3.1 Positivity and boundedness

Theorem 1. *All the solutions* $(S(t), E(t), A(t), I(t), Q(t), H(t), R(t), D(t), P(t)) \in \mathbb{R}^9_+$ *of the system (1) with primary conditions remain non negative and were uniformly bounded in the region* Ω *for all time* $t \geq 0$.

Proof 1. *Assumed that* $(S(t), E(t), A(t), I(t), Q(t), H(t), R(t), D(t), P(t)) \in \mathbb{R}^9_+$ *be a solution of (1) for* $t \in [0, t_0]$, *where* $t_0 \geq 0$.

From the equation (1.1),

$\frac{ds}{dt} = \Lambda - (\zeta_a A + \zeta_s I + \zeta_q Q)\frac{S}{N} - (\alpha + \mu)S \geq \Lambda - \phi(t)S$

where $\phi(t) = \beta(\zeta_a A + \zeta_s I + \zeta_q Q)\frac{S}{N} + (\alpha + \mu)$

$\Rightarrow \frac{ds}{dt} \geq \Lambda - \phi(t)S$

After integration, $S(t) = S^0 \exp(-\int_0^t \phi(s)\, ds) \int_0^t e^{\int_0^s \phi(u)\, du)} > 0$.

Hence, for all $t \in [0, t_0)$, *we get* $S(t) > 0$

From the equation (1.2),

$\frac{dE}{dt} = (\zeta_a A + \zeta_s I + \zeta_q Q)\frac{S}{N} - (\omega + \mu)E \geq -(\omega + \mu)E$

$\Rightarrow \frac{dE}{dt} \geq -(\omega + \mu)E$

$\Rightarrow E(t) \geq E^0 \exp(-\int_0^t (\omega + \mu)\, ds) \geq 0$

i.e, $E(t) \geq 0$

From the equation (1.3),

$\frac{dA}{dt} = \theta\omega E - (\lambda_a + \gamma_a + \mu_a + \mu)A \geq -(\lambda_a + \gamma_a + \mu_a + \mu)A$

$\Rightarrow \frac{dA}{dt} \geq -(\lambda_a + \gamma_a + \mu_a + \mu)A$

$\Rightarrow A(t) \geq A^0 \exp(-\int_0^t (\lambda_a + \gamma_a + \mu_a + \mu)\, ds \geq 0$

i.e,$A(t) \geq 0$

From the equation (1.4),

$\frac{dI}{dt} = (1 - \theta)\omega E - (\lambda_s + \eta_s + \mu)I \geq -(\lambda_s + \eta_s + \mu)I$

$\Rightarrow \frac{dI}{dt} \geq -(\lambda_s + \eta_s + \mu)I$

$\Rightarrow I(t) \geq I^0 \exp(-\int_0^t (\lambda_s + \eta_s + \mu)\, ds \geq 0$
$i.e, I(t) \geq 0$

From the equation of (1.5),

$\frac{dQ}{dt} = \lambda_a A + (\lambda_s I - (\eta_q + \gamma_q + \mu)Q \geq -(\eta_q + \gamma_q + \mu)Q$
$\Rightarrow \frac{dQ}{dt} \geq -(\eta_q + \gamma_q + \mu)Q$
$\Rightarrow Q(t) \geq Q^0 \exp(-\int_0^t (\eta_q + \gamma_q + \mu)\, ds \geq 0$
$i.e, Q(t) \geq 0$

From the equation (1.6),

$\frac{dH}{dt} = \eta_s I + \eta_q Q - (\gamma_h + \mu_h + \mu)H \geq -(\gamma_h + \mu_h + \mu)H$
$\Rightarrow \frac{dH}{dt} \geq -(\gamma_h + \mu_h + \mu)H$
$\Rightarrow H(t) = H^0 \exp(-\int_0^t (\gamma_h + \mu_h + \mu)\, ds \geq 0$
$i.e,\ H(t) \geq 0$

From the equation (1.7),

$\frac{dR}{dt} = \gamma_a A + \gamma_q Q + \gamma_h H - \mu R \geq \mu R$
$\Rightarrow \frac{dR}{dt} \geq \mu R$
$\Rightarrow R(t) \geq R^0 \exp(-\int_0^t \mu)\, ds \geq 0$
$i.e, R(t) \geq 0.$

Similarly we can prove that $D(t) \geq 0$ *and* $P(t) \geq 0$.

Hence $(S(t), E(t), A(t), I(t), Q(t), H(t), R(t), D(t), P(t))$ *of (1) with primary conditions for all* $t \in [0, t_0]$ *are non negative solutions in* Ω.

We prove that the boundedness of the solutions (S, E, A, I, Q, H, R,D,P) of system (1).

The positivity of the solutions implies that $\frac{dS}{dt} \leq \Lambda - (\alpha + \mu)S$.

From the above equation, we can write that

$\lim_{t\to\infty} supS \leq \frac{\Lambda}{(\alpha+\mu)}$ *and* $S \leq \frac{\Lambda}{(\alpha+\mu)}$.

consider the entire population $N = S + E + A + I + Q + H + R + D + P$.

By derivation of above equation gives $\frac{dN}{dt} \leq \Lambda - (\alpha + \mu)N$ *which leads to* $\lim_{t\to\infty} supN \leq \frac{\Lambda}{(\alpha+\mu)}$.

This implies that $N \leq \frac{\Lambda}{(\alpha+\mu)}$.

$S + E + A + I + Q + H + R + D + P \leq \frac{\Lambda}{(\alpha+\mu)}$.

Hence all the solution trajectories $(S(t), E(t), A(t), I(t), Q(t), H(t), R(t), D(t), P(t)$ *with primary conditions were uniformly bounded in the region*

$\Omega = (S(t), E(t), A(t), I(t), Q(t), H(t), R(t), D(t), P(t)) \in \mathbb{R}^9_+ : 0 \leq (S, E, A, I, Q, H, R, D, P) \leq \frac{\Lambda}{(\alpha+\mu)}$.

3.2 Basic reproduction number

The basic reproduction number, symbolized as R_0, was a prominent parameter in the analysis of contagious disease and it was defined as the total number of secondary cases arising through a primary case in susceptible individuals. If $R_0 > 1$ then the secondary cases were more than one, so that disease will continue in the population and become an epidemic. If $R_0 < 1$ then the secondary cases were less than one, so that disease cannot spread and die out as soon as possible. If $R_0 = 1$ then there is only one secondary case so that the disease is stable. Since at protection rate α population was protected, the susceptible individuals became $S = N(1 - \alpha)$. The disease-free equilibrium point $E^0 = (N(1-\alpha), 0, 0, 0, 0, 0, 0, 0, 0)$ of system (1) exists. Through Next Generation Matrix O.Diekmann et al [29] P.van den Driessche & Watmough [32] and Khajanchi, S et al [21], R_0 value will be calculated mathematically.

$$\mathcal{F} = \begin{pmatrix} \beta\zeta_a(1-\alpha) + \beta\zeta_s(1-\alpha) + \beta\zeta_q(1-\alpha) \\ 0 \\ 0 \\ 0 \\ 0 \end{pmatrix} \&\mathcal{V} = \begin{pmatrix} (\omega+\mu)E \\ -\theta\omega E + (\lambda_a + \gamma_a + \mu_a + \mu)I_a \\ -(1-\theta)\omega E + (\lambda_s + \eta_s + \mu)I_s \\ -\lambda_a I_a - (\lambda_s I_s + (\eta_q + \gamma_q + \mu)Q \end{pmatrix}$$

At disinfection state $E = A = I = Q = H = 0$,The Jacobian of two matrices $\mathcal{F}$ and $\mathcal{V}$ are

$$F = \begin{pmatrix} 0 & \beta\zeta_a(1-\alpha) & \beta\zeta_s(1-\alpha) & \beta\zeta_q(1-\alpha) \\ 0 & 0 & 0 & 0 \\ 0 & 0 & 0 & 0 \\ 0 & 0 & 0 & 0 \end{pmatrix}$$

$$V = \begin{pmatrix} \omega+\mu & 0 & 0 & 0 \\ -\theta\omega & \lambda_a + \gamma_a + \mu_a + \mu & 0 & 0 \\ -(1-\theta)\omega & 0 & \lambda_s + \eta_s + \mu & 0 \\ 0 & -\lambda_a & -\lambda_s & \eta_q + \gamma_q + \mu \end{pmatrix}$$

Therefore R_0 was obtained from equation $R_0 = \rho(FV^{-1})$,where ρ represented the matrix FV^{-1} spectral radius. Hence, the reproduction number was

$$R_0 = \frac{(1-\theta)\beta\omega\zeta_s(1-\alpha)}{(\lambda_s+\eta_s+\mu)(\omega+\mu)} + \frac{\beta\theta\omega\zeta_a(1-\alpha)}{(\lambda_a+\gamma_a+\mu_a+\mu)(\omega+\mu)} + \frac{\beta\zeta_q((1-\theta)(\lambda_a+\gamma_a+\mu_a+\mu)\omega\lambda_s+(\lambda_s+\eta_s+\mu)\theta\omega\lambda_a)(1-\alpha)}{(\lambda_a+\gamma_a+\mu_a+\mu)(\lambda_s+\eta_s+\mu)(\eta_q+\gamma_q+\mu)(\omega+\mu)} \quad (1)$$

3.3 Disease-free equilibrium Stability analysis

The Jacobian matrix J_{E^0} of the classification of equations (1) at the equilibrium point $E^0(\frac{\Delta}{\mu}, 0, 0, 0, 0, 0, 0, 0, 0)$ was
$J_{E^0} =$

$$\begin{pmatrix} -(\alpha+\mu) & 0 & -\beta\zeta_a(1-\alpha) & -\beta\zeta_s(1-\alpha) & -\beta\zeta_q(1-\alpha) & 0 & 0 & 0 & 0 \\ 0 & \omega+\mu & \beta\zeta_a(1-\alpha) & \beta\zeta_s(1-\alpha) & \beta\zeta_q(1-\alpha) & 0 & 0 & 0 & 0 \\ 0 & \theta\omega & -(\lambda_a+\gamma_a+\mu_a+\mu) & 0 & 0 & 0 & 0 & 0 & 0 \\ 0 & (1-\theta)\omega & 0 & -(\lambda_s+\eta_s+\mu) & 0 & 0 & 0 & 0 & 0 \\ 0 & 0 & \lambda_a & \lambda_s & -(\eta_q+\gamma_q+\mu) & 0 & 0 & 0 & 0 \\ 0 & 0 & 0 & \eta_s & \eta_q & -(\gamma_h+\mu_h+\mu) & 0 & 0 & 0 \\ 0 & 0 & \gamma_a & 0 & \gamma_q & \gamma_h & -\mu & 0 & 0 \\ \alpha & 0 & 0 & 0 & 0 & 0 & 0 & 0 & 0 \\ 0 & 0 & 0 & \mu_a & 0 & \mu_h & 0 & 0 & 0 \end{pmatrix}$$

The characteristic equation of the matrix J_{E^0} was $\mid J_{E^0} - \lambda I \mid = 0$
$(\lambda+\mu)(\lambda+(\alpha+\mu))(\lambda^9 + a_1\lambda^8 + a_2\lambda^7 + a_3\lambda^6 + a_4\lambda^5 + a_5\lambda^4 + a_6\lambda^3 + a_7\lambda^2 a_8\lambda + a_9) = 0$
where $a_1 = (A + G + J + K + t + E + I)$
$a_2 = (G+J+K)t + A(G+J+K+t+E+I) + (G+J+K+I+t)E + (G+J+K+E+t)I + BF + CH + G(J+K) + JK)$,
$a_3 = A(G+J+K+E+I)\mu + GE + JE + GI + KE + JI + KI + EI + BF + CH + GJ + GK + JK) + ... + I(J+K)\mu$,
$a_4 = A(GEI + JEI + KEI + BFJ + CGH + BFK + CHJ + CHK + GJK + (EI + BF + CH)\mu + ... + BFKI + GJKE + GJKI$,
$a_5 = A(FK\lambda_a D + GH\lambda_s D + HK\lambda_s D + (BFI + GJE + GKE + GJI + JKE + JKI + F\lambda_a D)\mu + ... + CHJKt + h\mu DII$,
$a_6 = A(BFJKI + GHK\lambda_s D + (BFJI + BFKI + GJKE + GJKI + FK\lambda_a D + GH\lambda_s D)\mu +$

$... + (FK\lambda_a DI + BFJKI)\mu$,
$a_7 = A(GJKEI + CGHJK + FK\lambda_a DI + BFJKI + GHK\lambda_s D)\mu$,
$a_8 = 0$ and $a_9 = 0$
Here $A = (\alpha + \mu)$,B=$\beta\zeta_a(1-\alpha)$ and $C = \beta\zeta_s(1-\alpha)$, $D = \beta\zeta_q(1-\alpha)$, $E = (\mu + \omega)$, $F = \theta\omega$,
$G = (\lambda_a+\gamma_a+\mu_a+\mu)$, $H = (1-\theta)$, $I = (\lambda_s+\eta_s+\mu)$, $J = (\eta_q+\gamma_q+\mu)$, $K = ((\gamma_h+\mu_h+\mu)$.
Hence J_{E^0} is singular because one of the eigenvalues is zero. Therefore at the disease-free equilibrium, the stability of the system (1) does not exists by using eigenvalues.

Theorem 2. *The Disease-Free Equilibrium* $E^0 = (\frac{\Lambda}{\mu}, 0, 0, 0, 0, 0, 0)$ *was locally asymptotically stable for* $R_0 < 1$ *and unstable for* $R_0 > 1$

Since the J_{E^0} has zero eigen value, according to Kermack WO [20] and singh HP[39], the theorem was satisfied that is the Disease-Free Equilibrium $E^0 = (\frac{\Lambda}{\mu}, 0, 0, 0, 0, 0, 0)$ was locally asymptotically stable for $R_0 < 1$ and unstable for $R_0 > 1$.

Table 2: Fitted parameters and their sensitivity indices list of SEAIQHRDP model

parameter	value	References	sensitivity indices
π	varies	-	-
ζ_a	0.4	Gumel AB et al.[12]	0.4547
ζ_s	0.4	Nadim SS et al.[27]	0.2416
ζ_q	0.3	Biswas, Sudhanshu Kumar et al [4]	0.3037
θ	0.7	Fergusonm.N et al. [10]	-0.0015
ω	0.1	R. Li et al. [36]	-0.1048
β	0.9714	evaluated	1.0000
α	0.0016	evaluated	-0.07158
λ_a	0.4614	evaluated	-0.1764
λ_s	0.1143	evaluated	-0.0997
η_s	0.1840	evaluated	-0.1418
η_q	0.0742	evaluated	-0.0948
γ_a	0.1302	evaluated	-0.2757
γ_q	0.1661	evaluated	-0.2088
γ_h	0.1777	evaluated	-0.2278
μ_a	0.0035	evaluated	-0.0207
μ_h	0.1544	evaluated	-0.0233
μ	0.0000391	Worldmeter.info/coronavirus [16]	-0.1070

4 Numerical simulation

In this sector, the numerical simulation of confirmed cases of COVID-19 for India was performed and the simulation results were compared with actual data [21] from 30^{th}, January 2020 to 13^{th}, January 2021. The SEAIQHRDP model fitted to daily and cumulative confirmed coronavirus cases in India which illustrates a satisfactory estimation. The model parameters β, α, λ_a, λ_s, η_s, η_q, γ_a, γ_q, γ_h, μ_a, μ_h and μ were estimated by using a nonlinear least squares regression method (LSQNONLIN function) in MATLAB.

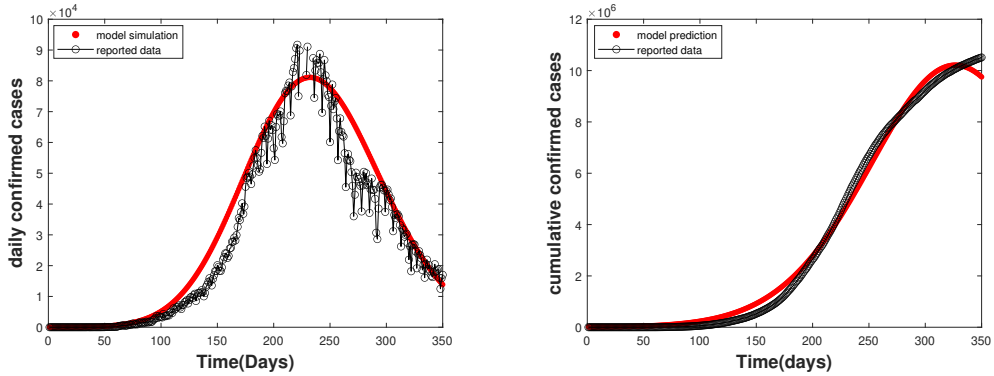

(a) (b)

Figure 2: The model fitting of reported (a) daily confirmed cases and (b) cumulative confirmed cases of COVID-19 in India.

The minimizing error was

$$R(\Phi) = \sum_{t=1}^{n} (Q_t(\Phi) - Q_t\bar{}(\Phi))^2 \tag{2}$$

where $Q_t(\Phi)$ and $Q_t\bar{}(\Phi)$ were a cumulative number of confirmed cases through actual data and model prediction. In Table 2, the values for the estimated and fixed parameters were shown. The fundamental reproduction numberR_0 was determined as 2.089 using the fixed and model parameters in Table 2.

In Figure.2 the curve fitting was taken from 30^{th}, January 2020 to 13^{th}, January 2021 in apicovid19india.org [13] in India. The black curve represented the reported COVID-19 cases and the red curve denoted the model simulation COVID-19 cases.

5 Sensitivity analysis

Sensitivity analysis was used in defining the impact of different factors in the spread of COVID-19. This analysis was used to identify the growth and reduction in basic reproduction numbers concerning numerous parameters. A complete chapter on the sensitivity analysis of the dengue virus was obtained in Rodrigues H et al. [37] and Burattini, M.N et al [6]. Whenever the significant parameters were recognized, different strategies will be executed to get optimum results. To identify such parameters, the sensitivity index of R_0 concerning various parameters was estimated. The normalized sensitivity index of R_0 is defined as

$$\Gamma_q^{R_0} = \frac{\partial R_0}{\partial q} \times \frac{q}{R_0}.$$

where q was the significant parameter, whose sensitivity on R_0 obtained by using normalized forward sensitivity index method Biswas, S et al [5].

The highest sensitive parameter on reproduction number was the parameter whose index was high in magnitude. If the sensitivity of parameter q was positive, R_0 was increased whenever the parameter q increased. Similarly, the sensitivity of parameter q was negative, R_0 was decreased whenever the parameter q increased. From Figure.3

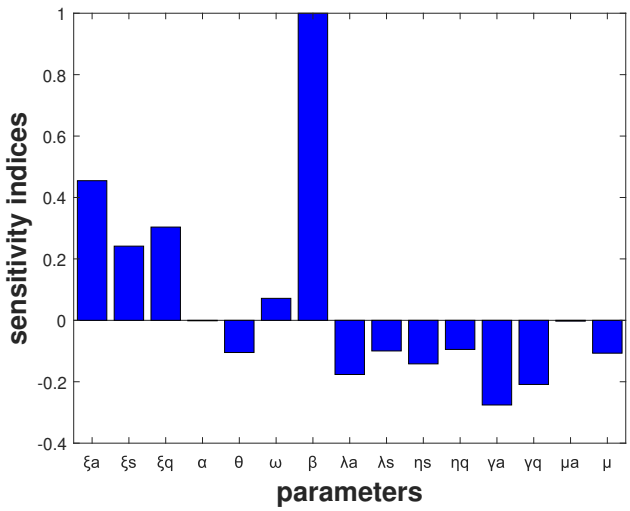

Figure 3: Normalized local sensitivity indices of R_0 with respect to each model parameter.

it was observed the parameters θ, λ_a, λ_s, η_s, η_q, γ_a, γ_q, μ_a have negative indices with R_0 and the parameters ζ_a, ζ_s , ζ_q, β, ω, μ share positive indices with R_0. So that R_0 value increased as the parameters ζ_a, ζ_s and ζ_q increased and R_0 value decreased as the parameters θ, η_s, η_q and γ_q increased. Hence the sensitive analysis determined that the parameters ζ_a, ζ_s, ζ_q, β, θ, η_s,γ_a and γ_q were more effective parameters. The sensitivity indices of various parameters had been displayed in Table 2.

Figure.4(a) represented that R_0 Contour Plot with respect to virus transmission rate (β) and quarantine rate (λ_s) from symptomatic population. This figure described a reduction in R_0 with a decrease in virus transmission rate (β) and an increase in quarantine rate (λ_s) from the symptomatic population. Figure.4(b) explained R_0 Contour Plot with respect to virus transmission rate (β) and hospitalization rate (η_s) from symptomatic population. This figure described a reduction in R_0 with a decrease in virus transmission rate β and an increase in hospitalization rate (η_s) from the symptomatic population. Figure.4(c) displayed R_0 Contour Plot with respect to quarantine rate (λ_a) from asymptomatic population and recovery rate (γ_q) from quarantine population. This figure demonstrated reduction in R_0 with an increase in quarantine rate (λ_a) from an asymptomatic population and an increase in recovery rate (γ_q) from quarantine population. Figure.4(d) expressed the Contour Plot of the Basic Reproduction Number concerning hospitalization rate (η_s) from symptomatic population and hospitalization rate (η_q) from quarantine population. This figure illustrated R_0 rises with a decrease in hospitalization rate (η_s) from the symptomatic population and hospitalization rate (η_q) from the quarantine population.

5.1 COVID-19 Prevalence changes with various parameters

From Figure.5 to Figure.9, It was perceived that the asymptomatic infected and symptomatic infected individuals were reduced if the protection rate (α) from susceptible individuals, quarantine rate (λ_a) from asymptomatic individuals, quarantine rate (λ_s) from symptomatic individuals, hospitalization rate (η_q) from quarantine individuals and hospitalization rate (η_s) from symptomatic individuals increased.

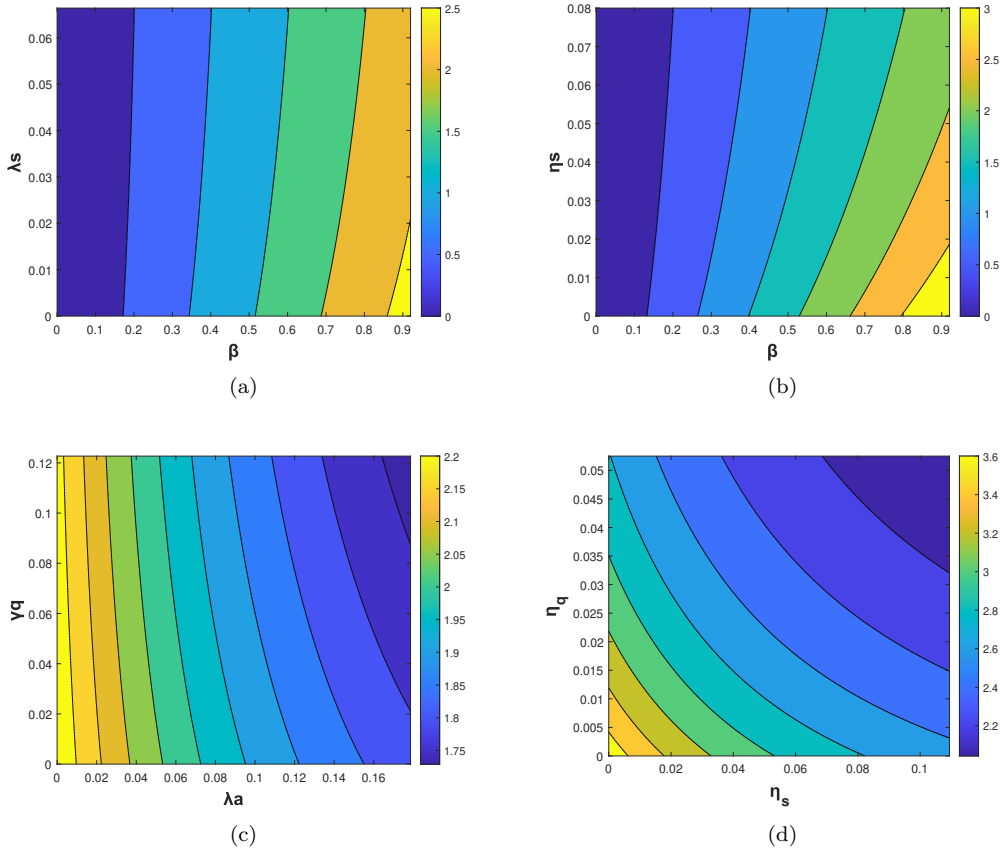

Figure 4: Contour plots of basic reproduction number R_0 with respect to (a) (β, λ_s), (b) (β η_s), (c) (λ_a, γ_q) and (d) (η_s, η_q).

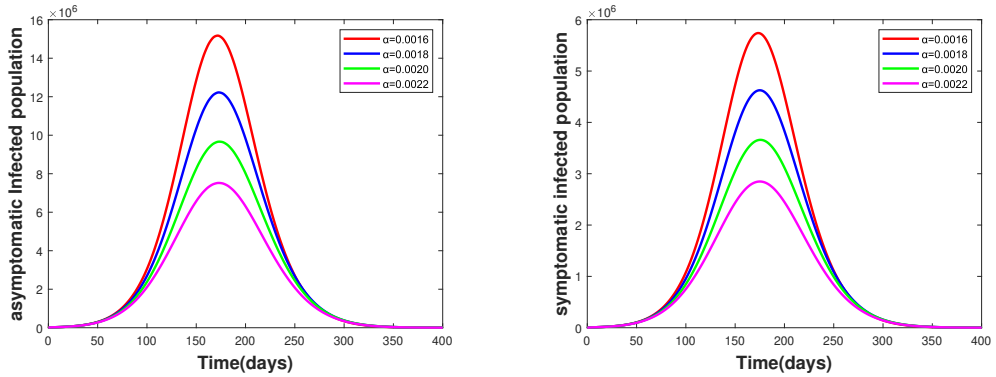

Figure 5: Effect of parameter α on (a) asymptomatic infected populace and (b) symptomatic infected populace

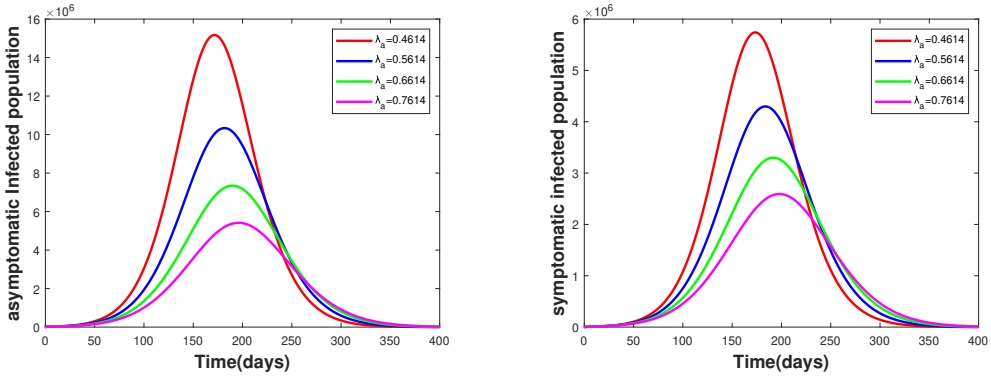

(a) (b)

Figure 6: Effect of parameter λ_a on (a) asymptomatic infected populace and (b) symptomatic infected populace

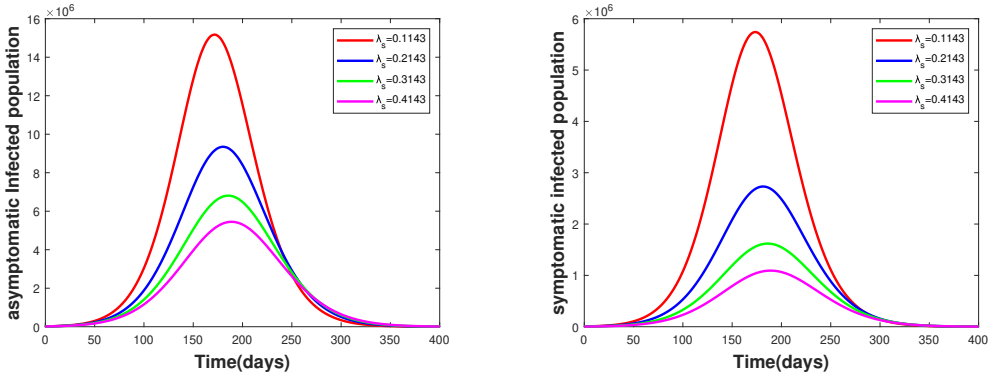

(a) (b)

Figure 7: Effect of parameter λ_s on (a) asymptomatic infected populace and (b) symptomatic infected populace

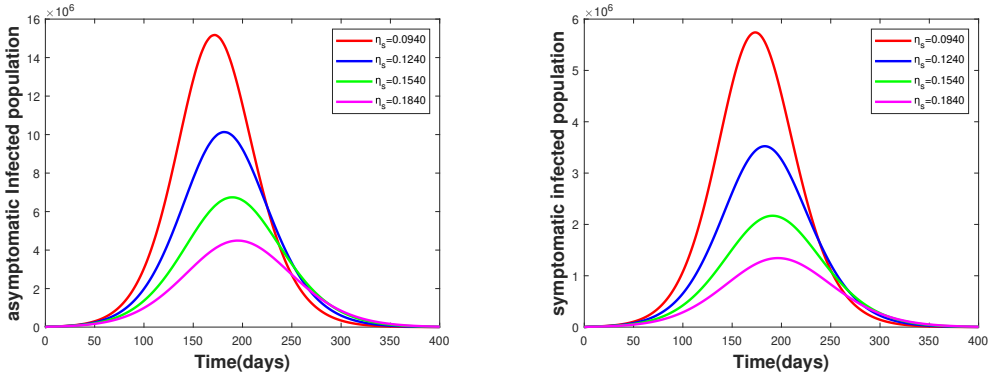

(a) (b)

Figure 8: Effect of parameter η_q on (a) asymptomatic infected populace and (b) symptomatic infected populace

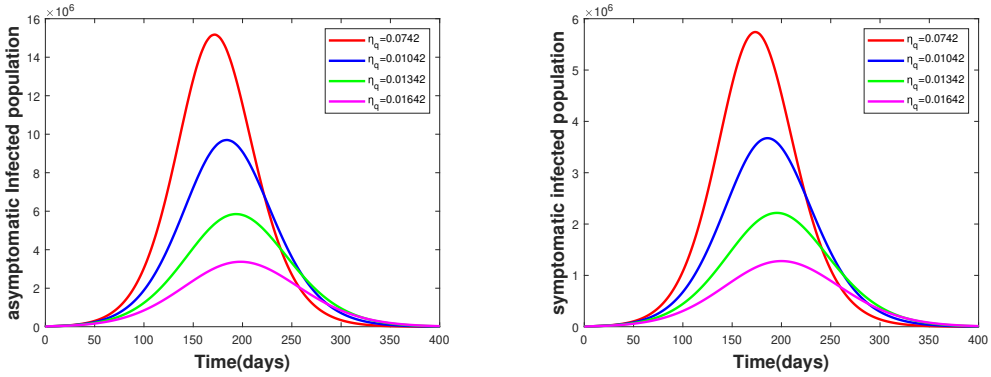

(a) (b)

Figure 9: Effect of parameter η_s on (a) asymptomatic infected populace and (b) symptomatic infected populace

6 Optimal control

6.1 Optimal control problem

The effectiveness of control techniques was crucial in decreasing the spread of the COVID-19 virus. It was essential to improve a policy that minimizes both the number of infected populations and related costs. In this phase, the optimal control technique was a tremendously useful tool for defining such a strategy. Now we study the impact of pharmacological interventions to diminish the spread of the virus. To achieve this, the system(1) can be extended by including three control variables $u_1(t)$, $u_2(t)$ and $u_3(t)$ where
(a) Control $u_1(t)$ represented the degree of protection provided by government interventions. The function of this control variable was to enhance the protection rate α.
(b) Control $u_2(t)$ described the treatment of asymptomatic infected individuals. The function of this control variable was to develop the quarantine rate (λ_a) from asymptomatic infected individuals.
(c) Control $u_3(t)$ characterized the treatment of symptomatic infected (both quarantine and hospitalization) individuals. The function of this control variable was to improve the quarantine rate (λ_s) and hospitalization rate (η_s) from symptomatic infected individuals. The three control variable values were assumed between 0 and 1.
There was no efforts made in these controls if $u_1 = u_2 = u_3 = 0$ and maximum efforts had been placed if $u_1 = u_2 = u_3 = 1$
By considering all the above suppositions, the optimal control model was formulated as

$\frac{ds}{dt} = \pi - \beta\frac{(\zeta_a A+\zeta_s I_s+\zeta_q Q)S}{N} - (\alpha + u_1 + \mu)S$
$\frac{dE}{dt} = \beta\frac{(\zeta_a A+\zeta_s I_s+\zeta_q Q)S}{N} - (\omega + \mu)E$
$\frac{dA}{dt} = \theta\omega E - (\lambda_a + u_2)A + \gamma_a + \mu_a + \mu)A$
$\frac{dI}{dt} = (1-\theta)\omega E - (\lambda_s + u_3 + \eta_s + u_3 + \mu)I$
$\frac{dQ}{dt} = (\lambda_a + u_2)A + (\lambda_s + u_3)I - (\eta_q + \gamma_q + \mu)Q$
$\frac{dH}{dt} = (\eta_s + u_3)I + \eta_q Q - (\gamma_h + \mu_h + \mu)H$
$\frac{dR}{dt} = \gamma_a A + \gamma_q Q + \gamma_h H - \mu R$
$\frac{dD}{dt} = \mu_a A + \mu_h H$
$\frac{dP}{dt} = \alpha S$

Now we detect $u_1(t)$, $u_2(t)$ and $u_3(t)$'s optimal values that minimize the objective functional
$\mathcal{J}(u_1(t), u_2(t), u_3(t))=\int_0^{t_f} (C_1 A + C_2 I + C_3 Q + C_4 H + \frac{1}{2}(C_5 u_1^2 + C_6 u_2^2 + C_7 u_3^2)\, dt$
subject to the system (2), which contained the sum of asymptomatic infected, symptomatic infected, quarantined, and hospitalized population, besides the optimal controls $u_1(t)$, $u_2(t)$ and $u_3(t)$. These were bounded and Lebesgue integral functions Kirschner D et al [9] and S. Lenhart and J.T.Workman [40]). Here The positive coefficients C_1, C_2, C_3, C_4, C_5, C_6 and C_7 were corresponding balancing weight constants parameters of stated infected variables and optimal controls.
The main purpose was to determine the optimal controls variables $u_1^*(t)$,$u_2^*(t)$,$u_3^*(t)$ such that

$$\mathcal{J}(u^*(t)) = \min_{u_1,u_2,u_3 \in U} \mathcal{J}((u_1(t), u_2(t), u_3(t))$$

where Φ= $\{u_1, u_2, u_3$: $u_1, u_2, u_3 /\ u_1, u_2, u_3 : [0, t_f] \to [0, 1]$ are lebsegue integrable$\}$.

Through Pontryagin's maximum principle Pontryagin, L et al [31], we derived the essential conditions for this optimal control problem. The Lagrangian function was given

by
$\mathcal{L}(S,E,A,I,Q,H,R,u_1(t),u_2(t),u_3(t)) = C_1A+C_2I+C_3Q+C_4H+\frac{1}{2}(C_4u_1^2+C_5u_2^2+C_5u_3^2$
The Hamiltonian function $\mathcal{H}$ obtained as
$\mathcal{H} = C_1A + C_2I + C_3Q + C_4H + \frac{1}{2}(C_4u_1^2 + C_5u_2^2 + C_5u_3^2 + \lambda_1\frac{dS}{dt} + \lambda_2\frac{dE}{dt} + \lambda_3\frac{dA}{dt} + \lambda_4\frac{dI}{dt} + \lambda_5\frac{dQ}{dt} + \lambda_6\frac{dH}{dt} + \lambda_7\frac{dR}{dt} + \lambda_8\frac{dD}{dt} + \lambda_9\frac{dP}{dt}$
where λ_1 λ_2, λ_3 , λ_4, λ_5, λ_6 and λ_7 are the adjoint variables.
The of differential equation form of adjoint variables were as follows.
$\frac{d\lambda_1}{dt} = -\frac{\partial\mathcal{H}}{\partial S} = (\lambda_1 - \lambda_2\beta(\frac{(\zeta_aA+\zeta_sI_s+\zeta_qQ)}{N} + (\lambda_1 - \lambda_8(\alpha+u_1) + \lambda_1u_1$
$\frac{d\lambda_2}{dt} = -\frac{\partial\mathcal{H}}{\partial E} = (\omega+\mu)\lambda_2 - \lambda_4 - \lambda_3\theta\omega - \lambda\omega$
$\frac{d\lambda_3}{dt} = -\frac{\partial\mathcal{H}}{\partial A} = -C_1 + (\lambda_1-\lambda_2)\beta\frac{\zeta_aS}{N} + (\lambda_3-\lambda_5)(\lambda_a+u_2) + ((\lambda_3-\lambda_8)\mu_a + \mu\lambda_3$
$\frac{d\lambda_4}{dt} = -\frac{\partial\mathcal{H}}{\partial I} = -C_2 + (\lambda_1-\lambda_2)\beta\frac{\zeta_sS}{N} + (\lambda_4-\lambda_5)(\lambda_s+u_3) + (\lambda_4-\lambda_6)(\eta_s+u_3) + \mu\lambda_4$
$\frac{d\lambda_5}{dt} = -\frac{\partial\mathcal{H}}{\partial Q} = -C_3 + (\lambda_1-\lambda_2)\beta\frac{\zeta_qS}{N} + (\lambda_5-\lambda_6)\eta_q + (\lambda_5-\lambda_7)\gamma_q + \mu\lambda_5$
$\frac{d\lambda_6}{dt} = -\frac{\partial\mathcal{H}}{\partial H} = -C_4 + (\lambda_6-\lambda_7)\gamma_h + (\lambda_6-\lambda_8)\mu_h + \mu)$
$\frac{d\lambda_7}{dt} = -\frac{\partial\mathcal{H}}{\partial R} = \mu\lambda_7$
$\frac{d\lambda_8}{dt} = -\frac{\partial\mathcal{H}}{\partial D} = 0$
$\frac{d\lambda_9}{dt} = -\frac{\partial\mathcal{H}}{\partial P} = 0$

we minimize Hamilton function relating to control variables $u_1^*(t)$,$u_2^*(t)$ and $u_3^*(t)$.
Using the optimal conditions $\frac{\partial\mathcal{H}}{\partial u_1} = 0$, $\frac{\partial\mathcal{H}}{\partial u_2} = 0$ and $\frac{\partial\mathcal{H}}{\partial u_3} = 0$, we get
$\frac{\partial\mathcal{H}}{\partial u_1} = C_5u_1 - \alpha\lambda_1 + \alpha\lambda_9S = 0 \Rightarrow u_1^* = \frac{(\lambda_1-\lambda_9)\alpha S}{NC_5}$
$\frac{\partial\mathcal{H}}{\partial u_2} = C_6u_2 - \lambda_3A + \lambda_5A = 0 \Rightarrow u_2^* = \frac{(\lambda_3-\lambda_5)A}{C_6}$
$\frac{\partial\mathcal{H}}{\partial u_3} = C_7u_3 - ((\lambda_4-\lambda_5+(\lambda_4-\lambda_6)I = 0 \Rightarrow u_3^* = \frac{((\lambda_4-\lambda_5)+(\lambda_4-\lambda_6))I}{C_7}$

6.2 Optimal control model simulation

With the values of the parameters mentioned in Table 2, numerical simulation was conducted for the optimal control problem (2) in MATLAB by using an iterative fourth-order Runge-Kutta method (Kamien, M et al [19] and Lukes, D.L.[24]) for the period [0,400]. The baseline weight parameters were taken as $C_1 = 1$, $C_2 = 1$, $C_3 = 1$, $C_4 = 1$,$C_5 = 40$, $C_6 = 40$ and $C_7 = 45$.

In Figure.10, variations of exposed, asymptomatic infected, symptomatic infected, quarantine, hospitalization, and dead populace with and without control had performed. This figure shows that, in comparison to the infected population without control, the infected population decreased quickly under control.

In Figure.11, variations of recovered and insusceptible Populace with and without control were executed. This graph demonstrates that the disinfected population under control swiftly rose in comparison to the disinfected population without control.

According to Figure.12, the best controls, u_1,u_2 and u_3 combined their efforts extremely well to increase the protection rate (α) from susceptible individuals, the quarantine rates (λ_a, λ_s)from asymptomatic infected and symptomatic infected individuals, and the hospitalization rates (η_q, η_s) from symptomatic and quarantine individuals.

From these figures we perceived that in the presence of optimal control strategy the number of susceptible, exposed, asymptomatic infected, symptomatic infected, quarantined, hospitalized, and dead individuals were reduced rapidly while the number of recovered and insusceptible individuals were increased swiftly comparing with the populations without control strategy.

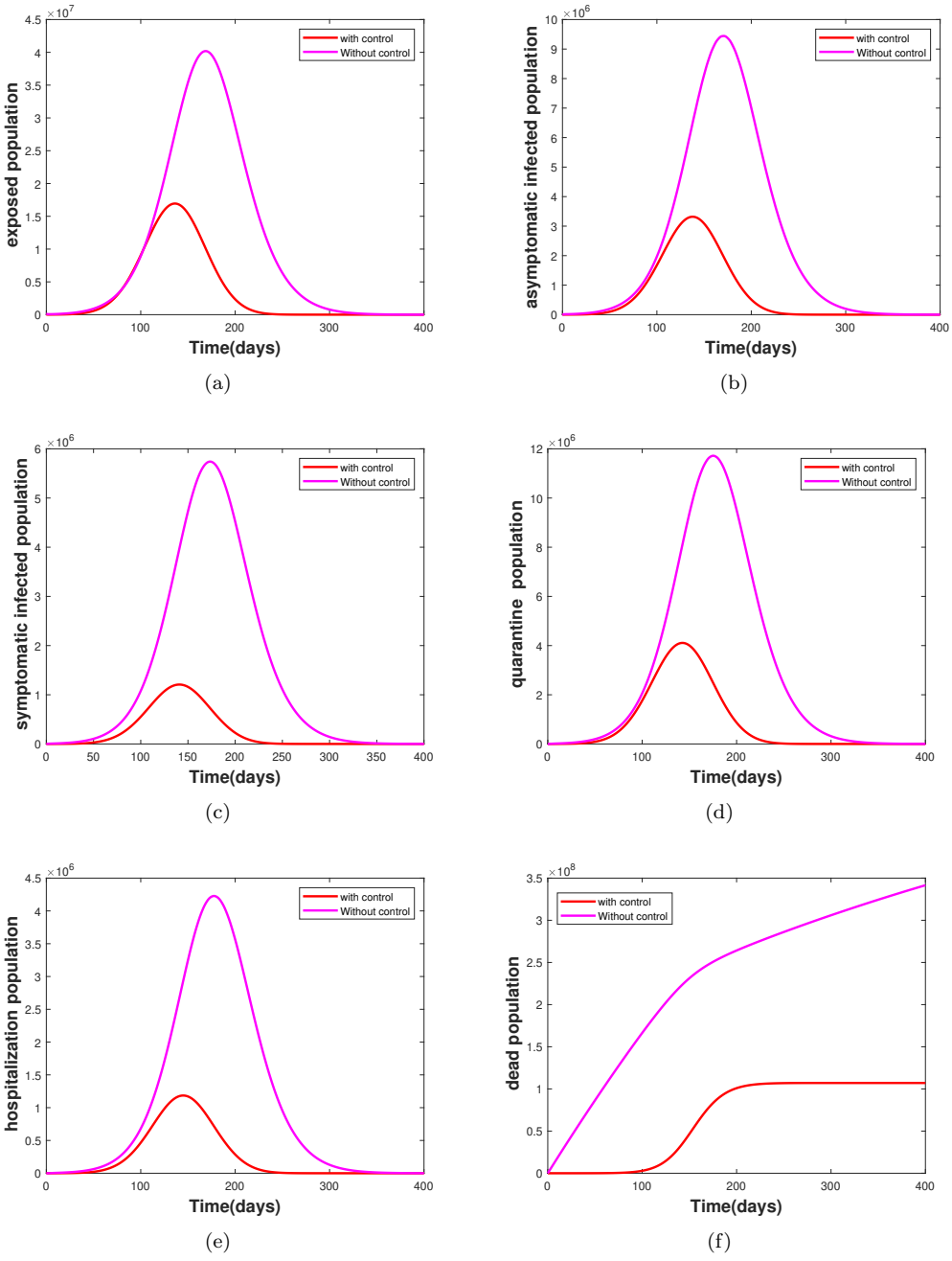

Figure 10: Variations of (a) exposed (b) asymptomatic (c) symptomatic infected (d) quarantine (e) hospitalization and (f) dead populations with and without control

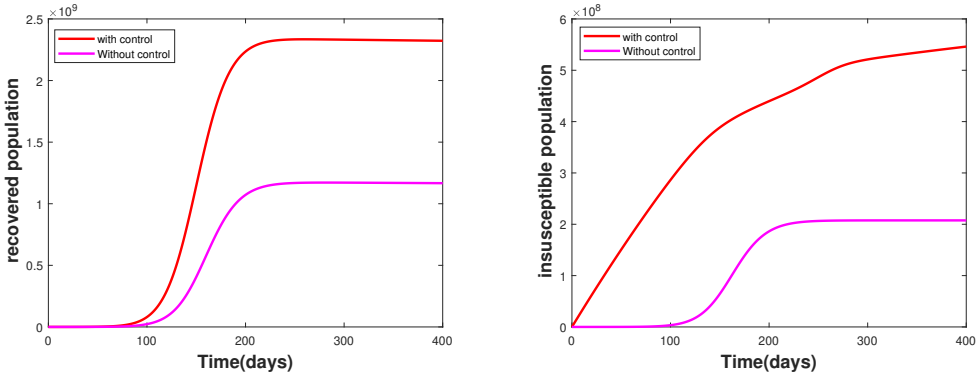

(a) (b)

Figure 11: Variations of (a) recovered (b) insusceptible population with and without control

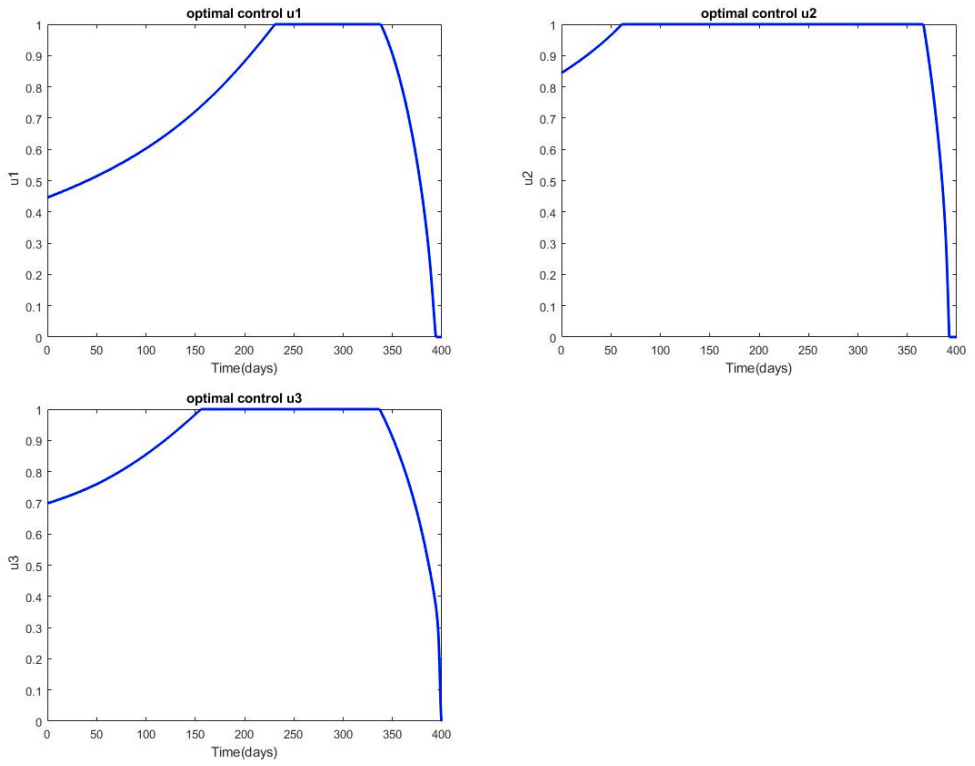

Figure 12: Dynamics of Optimal Controls u_1, u_2 and u_3

7 Conclusion

Epidemiological models aid in understanding the dynamics of infectious illness transmission. The deterministic mathematical model with 9 compartments was thoroughly studied in this paper. First, the elementary properties of the model such as the positivity and boundedness of the SEAIQHRDP model, the expression of R_0, and the local stability of the disease-free equilibrium were performed. Our suggested model has 18 parameters, but we only calculated 11 of them based on the sensitivity analysis. Through sensitivity analysis, it was observed that just eight parameters are very sensitive concerning clinically unwell or infected patients. The time series behavior of the infected populations for 400 days was examined concerning variations in parameters. From this, the spread of infections can be slowed down by increasing the protection rate, hospitalization rate, and quarantine rate. The best optimal control analysis was then carried out by including three control factors, one of which was increased protection, and the other two were improved quarantine and medical facilities for both identified and unidentified affected people. Through the Optimal control strategy, it was found that the infected populations were reduced rapidly, and disinfected populations were increased compared with the infected and disinfected populations without optimal control technique. When the best control approach is used early in a pandemic, the intensity of epidemic peaks tends to decline, spreading the maximum impact of an epidemic across a longer period. Finally, this study leads to the conclusion the rising of infections can be controlled only if the implementation of rapid testing, quarantine centers, and medical facilities. Additionally, we intend to increase the scope of our modeling work by including vaccination and the impact of environmental contaminants in the future.

References

[1] Alexander Krämer, Mirjam Kretzschmar, Klaus Krickeberg. "Krickeberg Modern Infectious Disease Epidemiology." 2010 : 209–221.(2010)

[2] Bai Y, Liu K, Chen Z. " Early transmission dynamics of novel coronavirus pneumonia epidemic in Shaanxi Province [J]." Chin J Nosocomiol 30(6):834–838(2020)

[3] Bandekar SR, Ghosh M." Mathematical modeling of COVID-19 in India and its states with optimal control." Model Earth Syst Environ. 2022;8(2):2019-2034. doi:10.1007/s40808-021-01202-8(2020)

[4] Biswas SK, Ghosh JK, Sarkar S, Ghosh U."COVID-19 pandemic in India: a mathematical model study." Nonlinear Dyn. 2020;102(1):537-553. doi:10.1007/s11071-020-05958-z(2020)

[5] Biswas SK, Ghosh U, Sarkar S. "Mathematical model of zika virus dynamics with vector control and sensitivity analysis.", Infect. Dis. Model. 5, 23–41 (2020)

[6] Brauer F, Chavez CC. "Mathematical models in population biology and epidemiology." Springer, New York, NY. https://doi. org/10.1007/978-1-4614-1686-9 (2012)

[7] Burattini MN, Massad E, Coutinho, FAB. "Estimation of R_0 from the initial phase of an outbreak of a vector-borne infection." Trop. Med. Int. Health 15(1), 120–26 (2010)

[8] Danane J, Hammouch Z, Allali K, Rashid S, Singh J. "A fractional-order model of coronavirus disease 2019 (COVID-19) with governmental action and individual reaction." Math Methods Appl Sci. 2021 Aug 25:10.1002/mma.7759. doi: 10.1002/mma.7759.(2021)

[9] D. Kirschner, S. Lenhart, S. Serbin. "Optimal control of the chemotherapy of HIV." Journal of Mathematical Biology, vol. 35, no. 7, pp. 775–792,(1997).

[10] Fergusonm.N et al Report 9: Impact of non-pharmaceutical interventions (NPIs) to reduce COVID19 mortality and healthcare demand, in https://doi.org/10.25561/77482 (2020).

[11] Giordano G, Blanchini F, Bruno R, Colanary P, Filippo AD, Matteo AD, Colaneri M. "Modelling the COVID-19 epidemic and implementation of population-wide interventions in Italy." Nat Med 26:855–860.(2020)

[12] Gumel AB, Ruan S, Day T, Watmough J, Brauer F, van den Driessche P, Gabrielson D, Bowman C, Alexander ME, Ardal S, Wu J, Sahai BM. "Modelling strategies for controlling SARS outbreaks." Proc Biol Sci. 2004 Nov 7;271(1554):2223-32. (2020)

[13] https://api.covid19india.org/documentation/csv/ Coronavirus outbreak in India. Google sheets

[14] https://www.who.int/director-general/speeches/detail/who-director-general-s-opening-remarks-at-the-media-briefing-on-COVID-19-11-march-2020

[15] https://covid19.who.int

[16] https://www.Worldmeter.info/coronavirus

[17] Huang G, Pan Q, Zhao S, Gao Y, Gao X. "Prediction of COVID-19 outbreak in China and optimal return date for university students based on propagation dynamics". J Shanghai Jiaotong Univ 25:140–146. (2020)

[18] H.W. Hethcote. "The mathematics of infectious diseases". SIAM Review 42.4 ,pp. 599-653. ISSN: 00361445(2000)

[19] Kamien, MI, Schwartz NL. "Dynamic Optimization: The Calculus of Variations and Optimal Control in Economics and Management". Modern Economy, Vol.11 No.7, July 15, 2020 (2020)

[20] Kermack WO, McKendrick AG "A contribution to the mathematical theory of epidemics". Proceedings of the London. Series A Contain Papers Mathematical Phys Charact 115(772):700–721 (1927)

[21] Khajanchi S, Bera S, Roy TK. "Mathematical analysis of the global dynamics of a HTLV-I infection model, considering the role of cytotoxic T-lymphocytes". Math. Comput.Simul. 180, 354–378 (2021)

[22] Lin Q, Zhao S, Gao D, Lou Y, Yang S, Musa S, Wang M, Cai Y, Wang W, Yang L. "A conceptual model for the outbreak of Coronavirus disease (COVID-19) in Wuhan, China with individual reaction and governmental action". Int J Infect Dis 93:211–216.(2020)

[23] Liu C, Ding G, Gong J, Wang L, Cheng K, Zhang D. "Studies on mathematical models for SARS outbreak prediction and warning". Chin Sci Bull 49(21):2245–2251(2004)

[24] Lukes DL. "Differential equations, classical to controlled". Mathematical Science Engineering 162. AcademicPress, New York (1982)

[25] Massad E, Coutinho FAB, Wilder-Smith A. Modelling an optimum vaccination strategy against ZIKA virus for outbreak use. Epidemiol Infect. 2019;147:e196. doi:10.1017/S0950268819000712(2019)

[26] Mwalili S, Kimathi M, Ojiambo V, Gathungu D, Mbogo R. "SEIR model for COVID-19 dynamics incorporating the environment and social distancing." BMC Res Notes. 2020 Jul 23;13(1):352(2020)

[27] Nadim SS, Ghosh I, Chattopadhyay J. "Short-term predictions and prevention strategies for COVID-19." A model-based study. Appl Math Comput. 2021 Sep 1;404:126251.(2021)

[28] NCBI: "First confirmed case of COVID-19 infection in India: a case report." https://www.ncbi.nlm.nih.gov/pmc/articles/ PMC7530459(2020)

[29] O. Diekmann, J. Heesterbeek, J. Metz. "On the definition and the computation of the basic reproduction ratio R_0 in models for infectious diseases in heterogeneous populations." J. Math. Biol. 28, 365–382 (1990)

[30] Peng L, Yang W, Zhang D, Zhuge C, Hong L. "Epidemic analysis of COVID-19 in China by dynamical modeling." medRxiv 2020.02.16.20023465; doi: https://doi.org/10.1101/2020.02.16.20023465(2020).

[31] Pontryagin, L.S., Boltyanskii, V.G., Gamkrelidze, R.V., Mishchenko, E.F. "The Mathematical Theory of Optimal Processes." Wiley-Interscience, New York (1962)

[32] P. van den Driessche, J. Watmough. "Reproduction numbers and sub-threshold endemic equilibria for compartmental models of disease transmission." Math. Biosci. 180(1–2), 29–48(2002)

[33] Raj Kishore, B.Sahoo, D.Swain, Kisor K. Sahu. "Analysis of COVID19 Outbreak in India using SEIR model." arXiv preprint arXiv:2010.13610 (2010)

[34] Read JM, Bridgen JR, Cummings DA, Ho A, Jewell CP. "Novel coronavirus 2019-nCoV: early estimation of epidemiological parameters and epidemic predictions." MedRxiv 2020.01.23.20018549; doi: https://doi.org/10.1101/2020.01.23.20018549 (2020)

[35] Rehman, Attiq ul, Ram Singh, Jagdev Singh. "Mathematical analysis of multi-compartmental malaria transmission model with reinfection." Chaos, Solitons and Fractals, volume 163, 112527, ISSN 0960-0779, https://doi.org/10.1016/j.chaos.2022.112527.(2022)

[36] R Li, Pei S, Chen B, Song Y, Zhang T, Yang W, Shaman J. "Substantial undocumented infection facilitates the rapid dissemination of novel coronavirus (SARS-CoV-2)." Science. 2020 May 1;368(6490):489-493. doi: 10.1126/science.abb3221(2020)

[37] Rodrigues H, Teresa M, Delfim F, Torres M. "Sensitivity Analysis in a Dengue Epidemiological Model." Conference Paper, Open Access Volume 2013, Article ID 721406, https://doi.org/10.1155/2013/721406(2013)

[38] RM May, Anderson RM. "Population biology of infectious diseases." Part II. Nature. 1979 Aug 9; 280(5722): 455-61. doi: 10.1038/280455a0. PMID: 460424(1979)

[39] Singh HP, Kumari p, Singh S. "SEIAQRDT model for the spread of novel coronavirus (COVID-19): A case study in India." Appl Intell (Dordr). 2021;51(5):2818-2837. doi: 10.1007/s10489-020-01929-4. Epub 2020 Nov 13. PMID: 34764566; PMCID: PMC7662031(2020)

[40] S. Lenhart, Workman JT. "Optimal Control Applied to Biological Models, Mathematical and Computational Biology Series." Chapman Hall CRC,(2007)

[41] Singh J, Ganbari B, Kumar D, Baleanu D. "Analysis of fractional model of guava for biological pest control with memory effect." J Adv Res. 2020 Dec 10;32:99-108. doi: 10.1016/j.jare.2020.12.004. PMID: 34484829; PMCID: PMC8408328(2020)

[42] Supriya Yadav, Devendra Kumar, Jagdev Singh, Dumitru Baleanu. "Analysis and dynamics of fractional order Covid-19 model with memory effect." Results in Physics, volume 24,2021, 104017, ISSN 2211-3797, https://doi.org/10.1016/j.rinp.2021.104017 (2021)